ELSEVIER

Polymer 42 (2001) 7025–7031

polymer

www.elsevier.nl/locate/polymer

Nanotribology of biaxially oriented poly(ethylene terephthalate) film

Ben D. Beake[a,1], Graham J. Leggett[a,*], Philip H. Shipway[b]

[a]*Department of Chemistry, The University of Manchester Institute of Science and Technology, PO Box 88, Manchester, M60 1QD, UK*
[b]*School of Mechanical, Materials, Manufacturing Engineering and Management, The University of Nottingham, University Park, Nottingham, NG7 2RD, UK*

Received 12 September 2000; received in revised form 28 February 2001; accepted 2 March 2001

Abstract

Repeated scanning of biaxially oriented poly(ethylene terephthalate) (PET) film surfaces in contact mode scanning force microscopy leads to sample wear. At low to moderate loads (<50 nN) well-defined ridges are formed. The dimensions and the separation of these ridges are determined by the scan parameters. The ridge spacing and the root mean squared (rms) roughness of the surface increase with the load, and appear to exhibit power law relationships. At low forces, material is not displaced from the scan area, but as the force is increased, increasing amounts of material are displaced to the periphery of the worn area. At high forces the surface disruption is extensive. The evolution of sample damage is not influenced by the scan rate, but is strongly influenced by changes in the number of scan lines, indicating that wear is a cumulative process, accelerated when the spacing between scan lines is small compared to the tip radius.

Keywords: Atomic force microscopy; Polyester; Nanotribology

1. Introduction

Polymer tribology is of increasing technological relevance as manufacturers design materials with carefully tailored mechanical and chemical properties for specific applications [1]. Although much progress has been made, a complete mechanistic understanding of the molecular processes which lead to the surface disruption has been frustrated by a lack of knowledge of the real area of contact and the fact that the modified area remains hidden during the wear testing. Recently, the advent of scanning force microscopy [2] and nanotribology [3–24] has provided a new approach. Nanotribology is the study of the microscopic surface properties and processes that contribute to material wear and consequent degradation of desirable properties. In a scanning force microscopy (SFM) experiment the tip can act as a model single-asperity contact, combining careful control of the applied force with in situ microscopic analysis of the modified region. Polymers and other soft materials are easily deformed during contact mode SFM imaging [25–39]. A periodic ridged wear pattern can be formed perpendicular to the direction of motion of the tip (the fast-scan axis) on repeat scanning of a wide variety of surfaces such as polystyrene (PS) [26–29], poly(methylmethacrylate) [30], poly(vinylchloride) [28], gelatin [31], poly(DL-lactide) [30], polyacetylene [32], polycarbonate (PC) (see Ref. [8], p. 280, [33,34]) and poly(ethylene terephthalate) (PET) [35–38]. No clear picture has yet emerged regarding the necessary conditions and mechanisms of ridge formation and the significance of their spacing, in part, possibly due to the contradictory findings reported in different studies. Meyers and co-workers found a strong interdependence between the orientation of the patterns formed by the tip [27], the applied load and the molecular weight (MW) of their amorphous PS samples. In contrast, Leung and Goh reported no dependence on MW [26], and although Woodland and Unertl noted that the wear resistance of their films increased with MW [29], they reported that the ridge spacing was independent of the applied load in their experiments. Elkaakour and co-workers observed that ridges formed immediately on drop-cast polyacetylene films and their spacing increased with applied load in the range 60–250 nN [32]. Jing and co-workers have reported that oriented patterns formed instantaneously on scanning the surface of amorphous PET. In comparison, patterns formed more slowly and were less clearly oriented perpendicular to the scan direction on annealed PET films [37]. The authors noted that the spacing between the ridges on the amorphous PET increased approximately linearly with load at the very low loads studied (0.1–1 nN).

* Corresponding author. Tel.: +44-161-200-4479; fax: +44-161-236-7677.

E-mail address: graham.leggett@umist.ac.uk (G.J. Leggett).

[1] Present address: Micro Materials Ltd, Unit 3, The Byre, Wrexham Technology Park, Wrexham LL13 7YP, UK.

0032-3861/01/$ - see front matter
PII: S0032-3861(01)00186-0

During our investigations into the frictional and adhesive properties of commercial PET films [38–44], we have determined the conditions necessary for wear-free imaging. Surface deformation on biaxially oriented PET film occurred at applied loads as low as 2 nN [38]. It was found that ridged structures formed after scanning for five cycles at applied loads as low as 10 nN. We have now considerably extended the scope of the work, and report a systematic investigation into the dependence and nature of the wear process on the operating parameters: applied load, cantilever stiffness, scan angle, scan speed, scan size and sampling density (the number of scan lines per unit area). We assess the various mechanistic models describing the tip-induced wear process in the light of our findings on the dependence of the wear pattern on the scanning parameters.

2. Experimental

The poly(ethylene terephthalate) film used in this study was Melinex 'O' obtained in sheet form with known processing conditions (ICI, Wilton, UK). It is a biaxially oriented additive-free PET film of low surface roughness.

Nanotribological experiments on the film surface were performed under ambient laboratory conditions with a Nanoscope IIIa MultiMode scanning probe microscope (Digital Instruments, UK) operating in contact mode. Imaging was performed using a range of silicon nitride cantilevers of varying stiffness (nominal normal force constants 0.06–0.58 N m^{-1}, NanoProbes from Digital Instruments) or silicon cantilevers (typical resonant frequency 68 kHz; nominal normal force constant ~2.8 N m^{-1}, NanoProbes from Digital Instruments). Force constants for individual silicon nitride cantilevers have been determined from measurements of their resonant frequency by a method implemented in the microscope software and based on the one originally reported by Cleveland et al. [45].

Tip-induced wear was performed by repeat scanning of an area of the film surface (typically 1×1 μm) at constant force. One scan cycle involves the acquisition of a complete image. The scan rate is equal to the scan frequency, and is related to the line-scan rate—i.e. it is the frequency of completion of individual line scans (where a single line scan involves a backwards–forwards sweep along a single line). The extent of the surface modification was then determined by re-imaging at lower imaging force and lower magnification (i.e. essentially non-perturbative conditions).

Unless specifically mentioned otherwise in the text, the parameters in a typical wear experiment were: 10 scan cycles, scan rate 55 Hz, 1×1 μm region, 512 scan lines, 90° scan angle (i.e. the with the axis of symmetry of the cantilever perpendicular to the fast scan axis), and the samples were placed in the microscope so that the direction of the initial draw of the biaxially oriented film was parallel to the fast-scan axis.

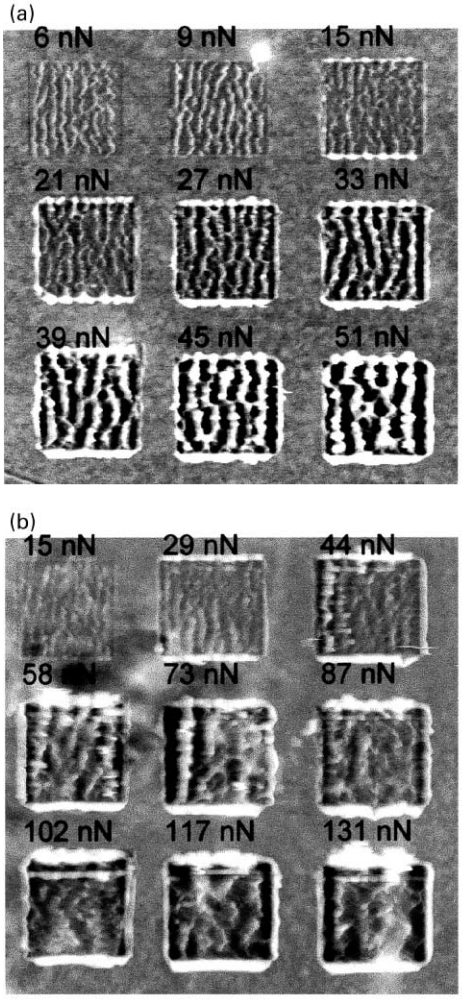

Fig. 1. (a) Topographic 5.5×5.5 μm image after the repeat-scanning nine 1×1 μm areas at different applied loads. Height range 0–25 nm. (b) Topographic 5.5×5.5 μm image after repeat-scanning nine 1×1 μm areas at different applied loads. Height range 0–80 nm.

3. Results

3.1. Applied load

Fig. 1 shows the effect of the applied load on the morphology developed during repeated scanning of specimens of Melinex O. Fig. 1(a) shows a 5.5×5.5 μm region containing nine 1×1 μm regions each of which has been scanned 10 times at different applied loads. A standard silicon nitride probe, with a cantilever spring constant of 0.13 N m^{-1} was employed. A ridged morphology is evident in all nine regions. Qualitatively, it may be seen that the ridges become more pronounced (higher and wider) as the load increases: after repeated scanning at a load of 6 nN, there are eight ridges running from top to bottom across the damaged

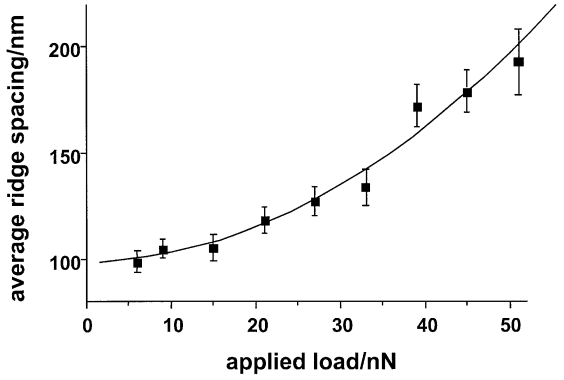

Fig. 2. Variation of ridge spacing with load.

region, and this number decreases to five at the highest load, 51 nN. In all cases, the direction of orientation of the ridges is the same: perpendicular to the scan direction. Not only do the heights of the ridge-tops increase with load, but the bottoms of the trenches that separate them become deeper, until at 51 nN they are significantly lower than the surrounding undamaged material. At the highest load, pronounced raised features are formed along the edges of the damaged region. These features most likely arise from the movement of material from the damaged region to its periphery. The size of these features decreases as the load decreases. They are just evident around the edge of the region scanned at a load of 15 nN, but are not evident after scanning at smaller loads.

Fig. 1(b) shows a further 5.5×5.5 μm region containing five 1×1 μm regions scanned 10 times at a range of loads. A stiffer cantilever (0.26 N m^{-1}) was employed here, giving access to a higher range of applied loads. It is clear that as the load becomes larger, the definition of the ridge features becomes reduced. While at the lowest loads they are very sharply defined, at loads of 100 nN and above they are broad and more poorly defined. When silicon probes with a cantilever force constant of 2.8 N m^{-1} were used, the loads were still higher and under these conditions, it was not possible to form ridged structures (although the surface disruption was severe).

It is useful to attempt to formulate some kind of quantitative measure of the extent of surface disruption due to repeated scanning. Fig. 2 shows the variation in the average ridge peak-to-peak separation as a function of load. It may be seen that the separation increases monotonically with load, in agreement with the qualitative conclusions drawn from Fig. 1. The data in Fig. 2 have been fitted with the relationship:

$$\text{average ridge spacing} = 98.79 + 0.07(\text{load}) + 0.04(\text{load})^2$$

Other workers have used the root mean square (rms) roughness to quantify the surface damage in studies of the repeated scanning of polystyrene [27–29]. In order to

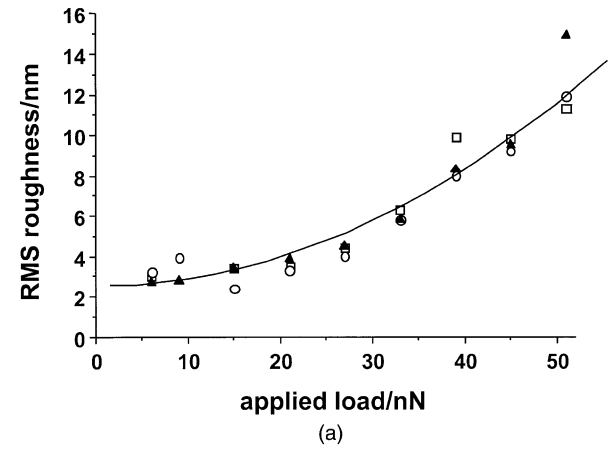

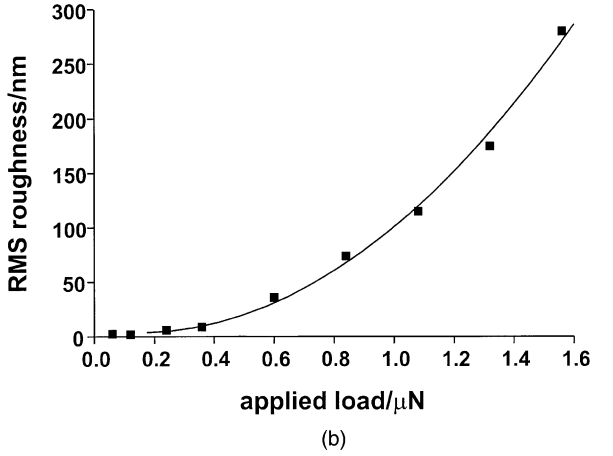

Fig. 3. (a) Variation in RMS surface roughness after 10 scan cycles with applied load for three different sets (squares, circles, triangles) of wear experiments with the same 0.13 Nm^{-1} probe tip. (b) Variation with the applied load of the RMS surface roughness (at 1.8×1.8 μm scale) after 10 scan cycles of a 3×3 μm area at 128 scan lines and 27.5 Hz, using a ~2.8 N m^{-1} silicon cantilever.

facilitate comparison with the results of these studies we have also measured the rms roughness of PET samples subjected to repeated scanning. While roughness is a simple measure of the surface topography, and does not directly provide insight into the mechanism of polymer modification, it is useful in the present context because it gives an indication of the way in which the undulation of the surface changes: it enables quantification of the extent of surface modification. Fig. 3 shows the relationship between rms roughness and the applied load in two regimes. The roughness was calculated for the central worn region but not for the surrounding region in which the material accumulated. The data for loads between 0 and 50 nN were recorded using a contact mode probe, with a cantilever stiffness of 0.13 N m^{-1}. These data (shown in Fig. 3(a)) may be fitted to a quadratic expression. The data in Fig. 3(b) were recorded using a stiffer probe, with a cantilever force constant of 2.8 N m^{-1}. At loads greater than 200 nN, the data fit a power-law relationship

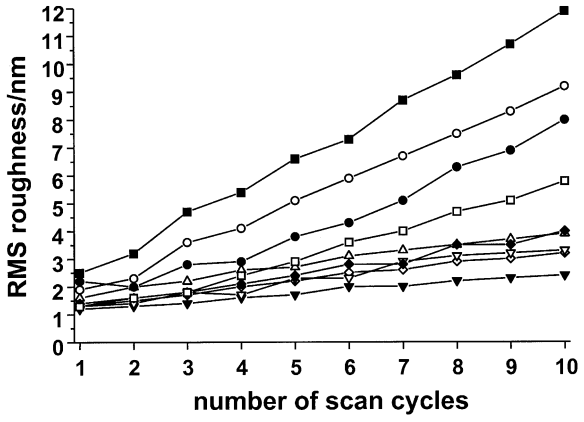

Fig. 4. Development of root-mean-square surface roughness with continued scanning at different applied loads. The applied loads were 6 nN, open diamonds; 9 nN, open up-triangles; 15 nN, closed triangles; 21 nN, open down-triangles; 27 nN, closed diamonds; 33 nN, open squares; 39 nN, closed circles; 45 nN, open circles; 51 nN, closed squares.

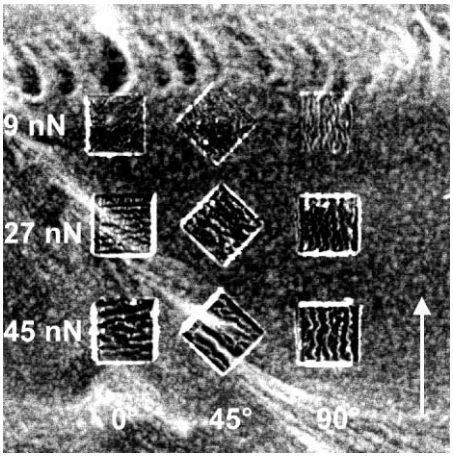

Fig. 5. Effect of scan angle on wear (a) Topographic 8 × 8 μm image after the repeat-scanning nine 1 × 1 μm areas at three different applied loads and scan angles. Image height contrast 0–20 nm. The arrow shows the machine direction.

of the form

$$\text{rms roughness} \propto (\text{applied load})^2$$

The rate of increase in the roughness appears steeper than that observed at lower loads, and the curve rises steeply towards high roughness values at loads above 1 μN. Although the rise in roughness appears to be unbounded at high loads, this may be an artefact of the algorithm used by the instrument software. Alternatively, it may be that a limiting roughness is reached at loads beyond the upper range accessible with our instrument. However, the general trends observed in the roughness-load relationship are clear.

Cantilevers with a wide range of force constants were utilised and a large range of loads was investigated. All of the findings were in agreement with the trends identified in Figs. 1–3.

3.2. Number of scan cycles

The number of scan cycles influenced the nature of the morphology after repeated scanning. The extent of surface disruption increased with the number of scan cycles. This is quantified in Fig. 4, which shows the rms roughness as a function of the number of scan cycles at a range of different loads. For all loads, the rms roughness increases monotonically with the number of scan cycles. Significantly, it is possible to generate a given degree of surface disruption with a variety of load-scan cycle combinations. For example, a mean ridge spacing of 130 nm, corresponding to an rms roughness of 4.5 nm, may be produced by scanning for eight cycles at 33 nN, six cycles at 39 nN or four cycles at 45 nN. Hence many cycles at a low load may produce the same surface structures that are generated by a much smaller number of cycles at a higher load.

3.3. Scan parameters

3.3.1. Scan angle

The sensitivity of the surface modification process to the direction of tip motion relative to the polymer draw directions during scanning was investigated. Fig. 5 shows nine regions, each of which have been scanned 10 times at three different loads and at angles of 0, 45 and 90° to the forwards draw direction of the polymer, which runs from top to bottom in the image. In all cases the result has been the formation of ridged structures perpendicular to the fast scan axis, and at all angles there is a tendency for material to be displaced to the periphery of the modified region of the surface. The image in Fig. 5 was recorded by imaging the area containing the nine modified regions at low force (i.e. notionally non-destructive conditions). However, the result after only one scan has been some reorientation of material in the regions worn at 45 and 90°. Generally, it was found that if ridges were created, and the area scanned again at a different angle, then the material in the ridges would be displaced with new ridges forming, after repeated scan cycles, orthogonal to the new scan direction. This indicates that the ridges are composed of material that is easily disrupted by the tip.

3.3.2. Scan size

For a given number of scan lines, the extent of wear was found to depend on the size of the scan area. Fig. 6 shows the results of an experiment where regions of differing size have been scanned 10 times at the same applied load and scan rate. The peak-to-peak separation of the ridges is greatest for the smallest region. Some typical data are given in Table 1, which shows roughness values for four different samples modified at a constant scan speed and fixed number of scan lines, but with different scan areas. It can be seen that there is a substantial change in the rms

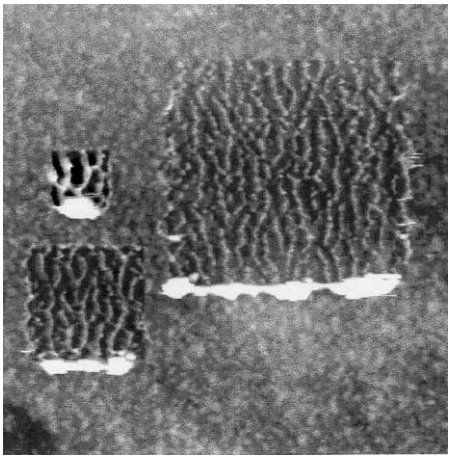

Fig. 6. Effect of scan size on wear, after 10 scans at 55 Hz with a 0.13 N m^{-1} cantilever at an applied load of 21 nN. Image height scale 0–30 nm.

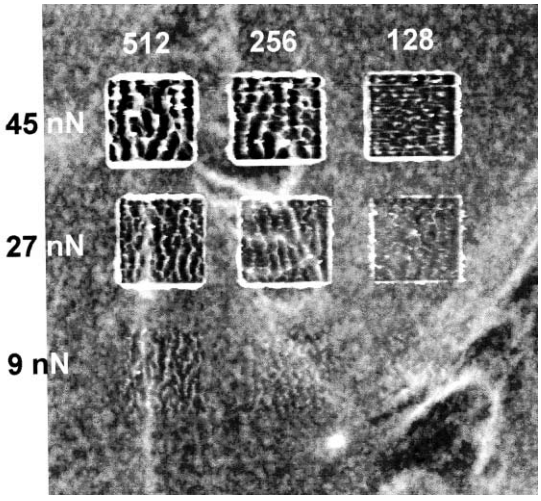

Fig. 7. Effect of the number of scan lines on wear. Topographic 6 × 6 μm image after the repeat-scanning of nine 1 × 1 μm areas at three different applied loads and numbers of scan lines with a 0.13 N m^{-1} cantilever. Image height scale 0–30 nm.

roughness, which is inversely proportional to the width of the scan area.

3.3.3. Sampling density

The number of scan lines was varied for a fixed area. Fig. 7 shows nine regions, the result of scanning at three different loads with 128, 256 and 512 lines per image. It can be seen that for a given load, the extent of disruption decreases with the number of scan lines. At a load of 45 nN, the disruption is substantial at 512 lines per image, but very much reduced at 128 lines per image.

3.3.4. Scan speed

The development of surface morphology was observed over a range of scan speeds, from 1 to 110 μm s^{-1}. No effect on the resulting surface morphology was observed, in agreement with the work of others. When the sample was rotated through 90°, so that the draw direction was rotated, and the experiment repeated, no change was observed in the morphology resulting from repeated scanning.

4. Discussion

Repeated scanning of Melinex O under a wide range of conditions led to the formation of a surface morphology composed of ridged structures separated by valleys. The bottoms of these valleys were below the level of the unmodified surface, and the peaks were raised above it. The ridged structures formed on Melinex O, a highly crystalline, oriented material, were qualitatively very similar to those observed on the surfaces of amorphous materials such as polystyrene [26–34]. While there were some minor differences between the structures of the features we observed on PET surfaces and those observed by others in studies of amorphous PS (in particular, those on PET are less straight and less continuous), it appears that the essential characteristics are very similar. It seems likely that these structures are a general feature of the interactions of AFM tips with polymeric materials. The absence of any dependence of the morphologies of the ridged structures on film orientation, as reported here and in a previous study [38], suggests that the mechanism of their formation is dependent largely on the scan parameters and is relatively insensitive to polymer surface microstructure.

Analysis of all of the data presented in the present study confirms that during the process of damage formation by repeated scanning, material is displaced by the tip to the peripheries of the scanned regions. In other words, the damage process is a wear process. The extent of the wear process may be gauged in a number of ways. Qualitatively, it is clear that increasing the load during scanning, or reducing the spacing between scan lines (by either reducing the scan area or increasing the number of lines per image) increases the size of the ridges. The spacing between the peaks of the ridges, and the depths of the troughs that separate them, also increase. In agreement with the suggestions of other workers [27,29], these changes may be readily correlated with changes in the rms roughness. In all cases, the amount of material displaced to the periphery of the scanned region increases with the measured parameter.

Table 1
Dependence of wear on scan area. Rms roughness after 10 scans with a 0.13 N m^{-1} cantilever at an applied load of 45 nN. Rms roughness measurements were taken over 400 × 400 nm areas

Scan area/nm	Scan rate/Hz	Rms roughness/nm
500 × 500	55	12.1
1000 × 1000	27.5	6.3
1500 × 1500	18.3	3.7
2500 × 2500	11	2.5
Unmodified surface		1.6 ± 0.2

The interaction of the tip with the PET surface causes plastic deformation of the surface. The process of wear formation is cumulative, and increasing the number of scan lines per region, or the load, leads to a greater accumulation of damage in a given number of scan cycles. However, a given amount of wear may be induced in a variety of ways: by using a high force and/or a small line spacing for a small number of cycles, or by using a small force and/or a larger line spacing for a larger number of cycles. While there are conditions under which the amount of wear is less than others, there does not appear to be a threshold below which one may be sure that no wear occurs; the best that can be hoped is to minimise the amount of plastic deformation.

The data in Fig. 7 clearly indicate that the closeness of the scan lines is a key parameter in the wear process. Successive scan lines may overlap; the closer the lines, the greater the overlap and hence the greater the degree of wear. Similar suggestions have been made by other workers. Elkaakour and co-workers made a similar observation during tip-induced modification of poly(acetylene) [32]. Schmidt and co-workers also found that the wear-induced features observed for amorphous PS melts varied with the number of scan lines [46,47]. Patterns became more closely aligned with the fast scan direction when the number of scan lines was increased. They suggested that portions of successive scans overlap, with the first pass softening the polymer and the second pass sweeping material towards the centre of the scan. This resulted in the formation of a raised ridge down the centre of the worn region. While overlapping of adjacent scans seems to be important in the present work, the explanation is probably different because the resulting wear-induced morphology is different (no pronounced, central ridge is observed). For the less mobile PET surface, sweeping is perhaps less important than for the more mobile PS surfaces studied by Schmidt et al.

The amount of wear (measured either by the spacing between ridges or the rms roughness) is related to both the load and the number of scan cycles by a power law, as proposed by Meyers et al. in their study of PS [27]. Woodland and Unertl excluded the possibility of a power law relationship in their study of PS, stating that in their work, the load and the ridge spacing are independent [29]. However, they gave no explanation for the difference between their findings and those of Meyers for nominally the same material. Our data demonstrate unequivocally that the ridge spacing and the load are related for PET, and lend support to the conclusions of Meyers et al.

Small deviations from the power law behaviour were observed at loads below 25 nN, when the rms roughness of the surface changed only little with decreasing load. The most likely explanation is that at these loads, the adhesive interaction between the tip and the sample is a substantial element of the resultant force acting at the surface. Measurements of the adhesion force performed at random locations on the surface revealed that it may be as great as 8 nN. The adhesive contribution may be expected to vary little with the applied load (it is thought that the capillary interaction is the major adhesive force), so that for loads greater than 25 nN, it becomes increasingly less significant. At low loads, this is not the case. It has been shown elsewhere that operation under water (thought to minimise adhesive interactions) leads to a substantial reduction in wear for relatively low loads when compared to the behaviour observed in ambient conditions, in agreement with this explanation.

We were not able to distinguish different regimes of wear behaviour, although there were substantial qualitative variations in the morphology resulting from wear. In their study of PS, Meyers et al. identified ‘abrasion’ patterns and ‘oriented’ patterns resulting from repeated scanning, which they correlated with differences in polymer molecular weight [27]. We observed structures similar to both types of pattern identified by Meyers et al., but there were no clear demarcation criteria that delineated conditions under which they were observed. The pattern described by Meyers et al. as an ‘oriented’ structure was generally observed under low damage conditions (small numbers of scans and/or low loads), consistent with their observation that such structures also formed after wear of high molecular weight materials, which were expected to be less easily disrupted. The pattern described as ‘abrasion’ was observed under more severe conditions (high loads and/or large numbers of scans, or close scan lines), consistent with the observation of Meyers et al. that such structures formed after wear of low molecular weight materials. The observation of a dependence of these morphologies on the scan conditions casts doubt on the interpretation presented by Meyers et al. that the abrasion pattern was characteristic of polymers with molecular weights less than the entanglement molecular weight. The molecular weight is only significant in that polymers with different molecular weights exhibit different susceptibilities to tip-induced plastic deformation, with the result that under specific conditions the wear induced may be more or less extensive.

Because of the range of behaviours observed under varying conditions in the present study, it would be erroneous to seek to define a characteristic or unique ridge spacing for a given material, as has been done previously by other workers. The surface roughness, ridge height and spacing all increased with continued scanning. However, there are nevertheless differences in behaviour between materials with different properties. Studies of uniaxially oriented PET specimens (not presented here) reveal a material that is softer, and exhibits a higher coefficient of friction, because of its lower level of crystallinity and orientation. Moreover, for polystyrene, Schmidt et al. observe radically different behaviour on heating the polymer above its glass transition temperature [46,47]. There may be other ways to quantify these changes. Given that the rms roughness and the ridge spacing varied with the load according to a power law, it may be possible to quantify the variation in these parameters for a range of materials and make comparisons

with their bulk mechanical properties and crystallinities. Ultimately, therefore, systematic studies of relationships between measures of the extent of damage and the loading conditions may reveal a way of utilising tip-induced wear data to reveal polymer tribological properties. The clear advantage of such an approach when compared to conventional, macroscopic tribological testing is that studies using the AFM enable nanoscale spatial resolution, creating the possibility of mapping tribological properties.

In the present study we found no dependence of the wear behaviour on the scan speed. For the entire range of scan frequencies accessible in an AFM, the speed of motion of the tip is slow. At 54.9 Hz, the tip velocity was only 110 $\mu m\ s^{-1}$. This finding is in contrast to the report by Woodland and Unertl [29], in which a linear relationship was reported between ridge spacing and scan speed for PS. However, the lowest scan speed used by these authors was greater than 100 $\mu m\ s^{-1}$, and at 80 $\mu m\ s^{-1}$ they reported that well-formed ridges were not observed. Vancso and coworkers found no dependence of wear on scanning speed for a nominally similar film material, in agreement with the present study [28], and in studies of the tip-induced wear of polycarbonate, Khurshudov and Kato also observed no scan-speed dependence, albeit at higher loads [33].

5. Conclusions

Under a wide range of conditions the repeat scanning of the polyester film surface with a scanning probe microscopy tip led to the formation of a tip-induced wear pattern comprising ridged structures and valleys, aligned perpendicular to the fast-scan axis. The surface roughness, height of the ridges and the spacing between them all increased with continued scanning. Both the spacing between the ridges and the rms roughness exhibited power law dependence on the load. Well-defined ridges were formed only at low to moderate load (below ~50 nN). Scanning at higher load led to more extensive surface disruption and the removal of much material to the periphery of the scan region.

Acknowledgements

We thank the EPSRC (grant GR/L78529) for financial support. Drs V. Vishnyakov (University of Salford, UK) and J.S.G. Ling (British Steel) are acknowledged for their contributions to this project in its early stages and for many useful discussions. Prof. D. Briggs (ICI, Wilton) is thanked for supplying Melinex 'O' with known processing history and for many helpful discussions.

References

[1] Zhang SW. Tribology Int 1998;31:49.
[2] Binnig G, Quate CF, Gerber C. Phys Rev Lett 1986;56:930.
[3] Bhushan B, Israelachvili JN, Landman U. Nature 1995;374:607.
[4] Kaneko R. Tribology Int 1995(28):195.
[5] Koinkar VN, Bhushan BJ. Vac Sci Technol A 1996;14:2378.
[6] Feldman K, Fritz M, Hähner G, Marti A, Spencer ND. Tribology Int. 1998;31:99.
[7] Feldman K, Hähner G, Spencer ND. Polym Prepr 1998;39:1148.
[8] Maganov SN, Whangbo M-H. Surface analysis with STM and AFM. Cambridge: VCH (UK) Ltd, 1996.
[9] Maganov SN, Reneker DH. Annu Rev Mater Sci 1997;27:175.
[10] Tsukruk VV. Rubber Chem Tech 1997;70:430.
[11] Overney RM, Meyer E, Frommer J, Brodbeck D, Lüthi R, Howald L, Güntherodt H-J, Fuijhira M, Takano H, Gotoh Y. Nature 1992;359:133.
[12] Meyer E, Overney RM, Brodbeck D, Howald L, Lüthi R, Frommer J, Güntherodt H-J. Phys Rev Lett 1992;69:1777.
[13] Tsukruk VV, Bliznyuk VN. Langmuir 1998;14:446.
[14] Tsukruk VV, Bliznyuk VN, Wu J. In: Ratner BD, Tsukruk VV, editors. ACS Symposium Series, vol. 694; 1998, p. 312.
[15] Bliznyuk VN, Everson MP, Tsukruk VVJ. Tribology 1998;120:489.
[16] Wilbur J, Biebuyck HA, MacDonald JC, Whitesides G. Langmuir 1995;11:825.
[17] Mate CM, IBM. J Res Develop 1995;39:617.
[18] Frisbie CD, Noy A, Rozsnyai LF, Wrighton MS, Lieber CM. Science 1994;265:2071.
[19] Frommer J. Thin Solid Films 1996;273:112.
[20] Overney RM, Bonner T, Meyer E, Rüetschi M, Lüthi R, Howald L, Frommer J, Güntherodt H-J, Fuijhira M, Takano HJ. Vac Sci Technol B 1994;12:1973.
[21] Carpick RW, Salmeron M. Chem Rev 1997;97:1163.
[22] Xiao X, Hu J, Charych DH, Salmeron M. Langmuir 1996;12:235.
[23] Bhushan B, Kulkarni AV, Koinkar VN, Boehm M, Odoni L, Martelet C, Belin M. Langmuir 1995;11:3189.
[24] Haugstad G, Gladfelter WL, Weberg EB, Weberg TT, Weatherill TD. Langmuir 1994;10:4295.
[25] Jin X, Unertl WN. Appl Phys Lett 1992;61:657.
[26] Leung OM, Goh MC. Science 1992;255:64.
[27] Meyers GF, DeKoven BM, Seitz JT. Langmuir 1992;8:2330.
[28] Vancso GJ, Allston TD, Chun I, Johnansson LS, Liu G, Smith PF. Int J Polym Anal Char 1996;3:89.
[29] Woodland DD, Unertl WN. Wear 1997;203-204:685.
[30] Gannepali A, Porter MD, Mallapragada SK, Abstr Pap Am Chem Soc 1998:215, No. Pt2, 002-PMSE.
[31] Domke J, Rotsch C, Hansma PK, Jacobson K, Radmacher M. In: Ratner BD, Tsukruk VV, editors. ACS Symposium Series 694, 1998, p. 178–93.
[32] Elkaakour Z, Aimé JP, Bouchacina T, Odin C, Masuda T. Phys Rev Lett 1994;73:3231.
[33] Khurshudov A, Kato K. Wear 1997;205:1.
[34] Jung TA, Moser A, Hug HJ, Brodbeck D, Hofer R, Hidber HR, Schwarz UD. Ultramicroscopy 1992;42-44:1446.
[35] Gould SAC, Schiraldi DA, Occeli MLJ. Appl Polym Sci 1997;65 1237.
[36] Gould SAC, Schiraldi DA, Occeli ML. Chem Tech 1998:35.
[37] Jing R, Henriksen PN, Wang H, Marteny PJ. Mater Sci 1995;30:5700.
[38] Ling JSG, Leggett GJ, Murray AJ. Polymer 1998;39:5913.
[39] Ling JSG, Leggett GJ. Polymer 1997;38:2617.
[40] Beake BD, Ling JSG, Leggett GJ. J Mater Chem 1998;8:1735.
[41] Beake BD, Ling JSG, Leggett GJ. J Mater Chem 1998;8:2845.
[42] Beake BD, Ling JSG, Leggett GJ. Polymer 1999;40:5973.
[43] Beake BD, Ling JSG, Leggett GJ. Polymer 2000;41:2241.
[44] Beake BD, Leggett GJ, Shipway PH. Surf Interface Anal 1999;27:1084.
[45] Cleveland JP, Manne S, Bocek D, Hansma PK. Rev Sci Instrum 1993;64:403.
[46] Schmidt RH, Haugstad G, Gladfelter WL. Polym Prepr 1998;39(2):1159.
[47] Schmidt RH, Haugstad G, Gladfelter WL. Langmuir 1999;15:317.